Applied Catalysis B: Environmental 138–139 (2013) 276–284

Contents lists available at SciVerse ScienceDirect

Applied Catalysis B: Environmental

journal homepage: www.elsevier.com/locate/apcatb

Fe/SiO_2 heterogeneous Fenton catalyst for continuous catalytic wet peroxide oxidation prepared *in situ* by grafting of iron released from $LaFeO_3$

G. Satishkumar[a,b,*], M.V. Landau[b,*], T. Buzaglo[b], L. Frimet[b], M. Ferentz[b], R. Vidruk[b], F. Wagner[c], Y. Gal[b], M. Herskowitz[b]

[a] Center for Excellence in Nanomaterials, Materials Chemistry Division, School of Advanced Sciences, VIT University, Vellore-632 014, Tamil Nadu, India
[b] Blechner Center for Industrial Catalysis and Process Development, Department of Chemical Engineering, Ben-Gurion University of the Negev, Beer-Sheva 84105, Israel
[c] E15 Physic Department TVM Technische Universität, München, Garching 6, München, Germany

ARTICLE INFO

Article history:
Received 22 September 2012
Received in revised form 18 February 2013
Accepted 21 February 2013
Available online 1 March 2013

Keywords:
$LaFeO_3$ perovskite
Selective extraction-deposition
Silica
Isolated iron ions
Phenol wet peroxide oxidation

ABSTRACT

Functionalization of silica-gel by immobilization of iron ions at its surface was carried out through a novel method – selective extraction–deposition (SED) in acidic solution using $LaFeO_3$ orthoferrite with perovskite structure as a solid precursor. Isolated Fe-ions produced as a result of precursors decomposition in acidic aqueous solution were trapped by silica surface silanols. The presence of iron in the only one state of isolated surface ions over 2 wt%Fe/SiO_2 material at the Fe content corresponded to surface silanols concentration was confirmed using ESR, Mossbauer spectroscopy, UV Raman, FTIR and XPS techniques. Catalytic performance of 2 wt% Fe/SiO_2 was examined toward catalytic wet peroxide oxidation (CWPO) of phenol in up flow fixed bed reactor at pH 4, 80 °C, LHSV 6 h^{-1} with 200 ppmw phenol and 1300 ppmw hydrogen peroxide in water. It was demonstrated that mixing of $LaFeO_3$ with silica-gel gives an advanced catalytic material with high activity (TOC removal of 90%) and stability without iron leaching. This effect is due to dynamic behavior of iron that includes its SED–leaching–condensation along the catalysts layer. In this case, the $LaFeO_3$ has a multiple function–active catalytic component, precursor of iron ions and buffer controlling the pH along the catalysts layer.

1. Introduction

Fenton catalytic wet oxidation with hydrogen peroxide (CWPO) is an efficient method for purification of industrial wastewater from organic contaminants at atmospheric pressure and low temperatures of 50–80 °C [1]. The soluble homogeneous iron catalyst is used at pH = 3 and high H_2O_2 concentrations (Fe/H_2O_2 = 1/5) requiring neutralization/separation of treated water by complex methods [1,2]. Many attempts have been done to test the efficiency of iron species immobilized in solid matrices as heterogeneous (solid) Fenton catalysts in batch reactors [3–5]. For example, mixed Al–Fe pillared clays prepared from bentonite were reported to be efficient catalyst in the CWPO of phenol with iron leaching of less than 0.2 wt% of the total initial iron content [4,5]. The authors concluded that isolated iron species in the catalyst pillared by Al–Fe mixed complexes are very active sites for CWPO of phenol. Only a few catalysts were experimented in fixed-bed reactors using phenol as a model contaminant yielded a maximum TOC conversion of 70% [6–8]. Leaching of iron was in all the cases detected from 18 ppmw (9.2%)[7] to 123 ppmw (32%) [8].

The strong deactivation caused by iron leaching at pH = 3 diminished the conversion after about 8–10 h on run [7]. Development of an efficient CWPO process with a solid Fenton catalyst is still a challenge. The main reason for relatively low activity of reported solid Fenton catalysts is the existence of active iron in form of oxide clusters and nanocrystals. This is due to hydrolysis and self-condensation of iron ions into colloids and even precipitates in precursors solutions rendering very low loading (i.e. ~0.2 μmol/m^2 SiO_2) of isolated Fe-ions by adsorption [9]. The condensed iron species have low catalytic activity since the neighboring Fe ions in condensed species scavenge $^{\bullet}OH$ radicals [10,11]. Increasing pH reduces iron leaching but is limited by decreasing the activity since protons participate in the redox cycle producing active $^{\bullet}OH$ radicals [12].

* Corresponding authors at: Center for Excellence in Nanomaterials, Materials Chemistry Division, School of Advanced Sciences, VIT University, Vellore-632 014, Tamil Nadu, India/Blechner Center for Industrial Catalysis and Process Development, Department of Chemical Engineering, Ben-Gurion University of the Negev, Beer-Sheva 84105, Israel. Tel.: +91 4162243092.
E-mail addresses: satishkumar.g@vit.ac.in, satishgsamy@yahoo.co.in (G. Satishkumar), mlandau@bgu.ac.il (M.V. Landau).

0926-3373/$ – see front matter © 2013 Elsevier B.V. All rights reserved.
http://dx.doi.org/10.1016/j.apcatb.2013.02.040

Hence immobilization of isolated iron ions at the surface of a suitable support would be good strategy to prevent the self condensation of iron ions. In this case every iron ion will serve as an active site producing $^{\bullet}OH$ radicals without their recombination at the neighbor iron sites as in the case of iron oxide-hydroxide clusters and nanoparticles. Stabilizing of isolated iron ions on the surface of suitable high-surface area support like silica-gel is a challenge due to fast hydrolysis and condensation of iron ions in solutions of Fe-precursors (salts, alkoxides, etc.) used for catalysts preparation [9]. The reported successful attempts for preparation of such solids were done by co-condensation of iron and silicon precursors with restricted ability to control the extent of Fe ions self-condensation and location at the surface of pore walls or in the bulk of the solid material [13,14].

In the present work, the proposed technical solution permits deposition of isolated iron ions on high-surface area supports like silica-gel through selective extraction deposition (SED) method using $LaFeO_3$ perovskite as a solid precursor. The same catalyst was also prepared *in situ* by treating perovskite and silica-gel mixture with acidic solution inside the tubular catalytic reactor. Catalytic wet oxidation experiments in presence of hydrogen peroxide using phenol as a model pollutant were carried out in up-flow fixed bed reactor. Under the same reaction conditions was examined catalytic performance of silica-gel functionalized with isolated surface iron ions, pure $LaFeO_3$ perovskite, bulk iron compounds hematite and goethite and a mixed $LaFeO_3$–SiO_2 material where SED of iron ions proceeded continuously during the catalytic run. The last mixed material displayed highest efficiency that allowed achieving of 90% TOC conversion for 100 h without leaching of iron. Such performance combining close to complete TOC removal with continuous operation for a long period was obtained for the first time with a solid Fenton catalyst demonstrating high potential of surface-functionalized materials for this purpose.

2. Experimental

2.1. Preparation of catalytic materials

2.1.1. Synthesis of $LaFeO_3$

The $LaFeO_3$ perovskite was synthesized according to procedure developed in [15]. Equal amounts of moles of Iron nitrate $Fe(NO_3)_3{\cdot}9H_2O$ (Strem Chemicals) and Lanthanum nitrate $La(NO_3){\cdot}6H_2O$ (Merk) (8.86×10^{-3} mol) were dissolved separately in 15 ml of water by stirring for 15 min at r.t., after which the two solutions were mixed together and stirred for additional 30 min. 0.048 mol of Glycine (Sigma Aldrich) was added and the solution was mixed for another 30 min. Then the solution was evaporated under stirring at 80 °C until gelation occurred. Combustion was carried out in air at 200 °C (heating rate: 10 °C/min) for 2 h and then was conducted calcination under air flow at 600 °C for 4 h (heating rate: 5 °C/min, flow rate: 10 ($L/h \times g$)).

2.1.2. Synthesis of 2 wt% Fe/SiO_2 by SED strategy

The target of SED technique is to immobilize isolated iron ions at the silica surface by grafting using their co-condensation with surface silanols that ensures the surface location of Fe-ions. The idea was to use a solid precursor $LaFeO_3$ – the lanthanum ferrite salt with perovskite structure as a precursor of iron ions in aqueous suspension of silica. It was agitated with silica in acidic solution (pH = 3, H_2SO_4) that extracted iron ions from perovskite precursor:

$$2LaFeO_3 + 3H_2SO_4 \rightarrow La_2(SO_4)_3 + 2Fe(3+) + 6H(+) + 6O(2-) \quad (1)$$

allowing them to condense with surface silanols by three different routes:

$$2Fe(3+) + 6H(+) + 6O(2-) + 2Si{-}OH \rightarrow 2O{=}Fe{-}O{-}Si + 4H_2O \quad (2)$$

$$2Fe(3+) + 6H(+) + 6O(2-) + 4Si{-}OH \rightarrow 2(HO)Fe(O{-}Si)_2 + 4H_2O \quad (3)$$

$$2Fe(3+) + 6H(+) + 6O(2-) + 3Si{-}OH \rightarrow 2Fe(O{-}Si)_3 + 6H_2O, \quad (4)$$

that yields mono- bi- and tridentate surface complexes of iron ions.

This minimizes the residence time and concentration of iron ions in the solution avoiding polycondensation (self-condensation) of Fe-ions [9]. The iron ions released to the acidic solution immediately reacted with surface silanols. The selection of La-perovskite as a Fe-precursor was based on the following considerations: (i) It is highly reactive in acidic solution at pH = 3, (ii) The iron and lanthanum ions (M^{n+}) have very different affinity to surface silanols at pH > isoelectric point of silica (pH_{IEP} = 2.2 was measured for silica-gel used in this work based on electroforetic mobility at 25 °C with Malvern-Zetamaster instrument of ZEM type). The ion-exchange equilibrium is established according to reaction (5) with pK_{Fe} = 3.7 and pK_{La} = 15 [16]. Together with the changes

$$[n\mathrm{Si}{-}\mathrm{OH}]_S + M^{n+} \longleftrightarrow [M(O{-}Si)_n]_S + nH^+ \quad (5)$$

of entropy estimated for reaction (5): ΔS°_{Fe} = 9.5 kcal/mol K; ΔS°_{La} = −73.6 kcal/mol K [16], this should cause selective adsorption of Fe-ions at silica surface. It was expected that iron ions will be adsorbed at the surface of silica matrix at loading corresponded to the surface concentration of silanols while lanthanum will remain in the solution.

A mixture of 0.5 g $LaFeO_3$ (20 nm nanocrystals) and 5 g of silica-gel was added to the 500 cm^3 of diluted aqueous H_2SO_4 (Frutarom) at 80 °C and pH = 3.0 maintaining negative charging of silica surface. $LaFeO_3$ was in form of porous 30–150 μm aggregates with surface area of 41 m^2/g. Silica represented 20–150 μm particles of silica-gel PQEP10X CS5717 (PQ Corp.) with surface area of 314 m^2/g, PV = 1.9 cm^3/g and BD = 0.24 g/cm^3 containing 0.68 mmol of silanols per gram according to surface titration [17]. On stirring due to decomposition of perovskite at acidic conditions the pH of the solution increases from 3 to 4.5. In order to decompose all the perovskite pH of the solution was maintained at 3 by adding dilute 0.1 M sulphuric acid externally. Stirring was stopped when there was no further increase of solution pH indicating the complete decomposition of perovskite. The solid was separated by filtration, washed with distilled water and dried in air at 100 °C overnight.

2.1.3. Synthesis of Fe_2O_3–FeOOH–NP through SED technique

Treatment of $LaFeO_3$ with H_2SO_4 solution maintaining pH at the level of 3.0 as in the case of synthesis of 2 wt%Fe/SiO_2 material, in the absence of silica gel yielded a precipitate containing nanoparticles of Fe_2O_3 and FeOOH formed according to Eqs. (6) and (7):

$$2LaFeO_3 + 3H_2SO_4 \rightarrow La_2(SO_4)_3 + Fe_2O_3 + 3H_2O \quad (6)$$

$$2LaFeO_3 + H_2SO_4 \rightarrow La_2(SO_4) + 2FeOOH + 2H_2O \quad (7)$$

2.1.4. Synthesis of 6 wt% $Fe(LaFeO_3)$–SiO_2 in situ by SED strategy

The 6 wt% $Fe(LaFeO_3)$–SiO_2 catalyst was prepared *in situ* by packing a mechanical mixture of 720 mg silica-gel (3 cm^3) and 260 mg $LaFeO_3$ between two beds of glass Rashing rings 3 mm × 3 mm separated by glass wool in a tubular SS reactor with

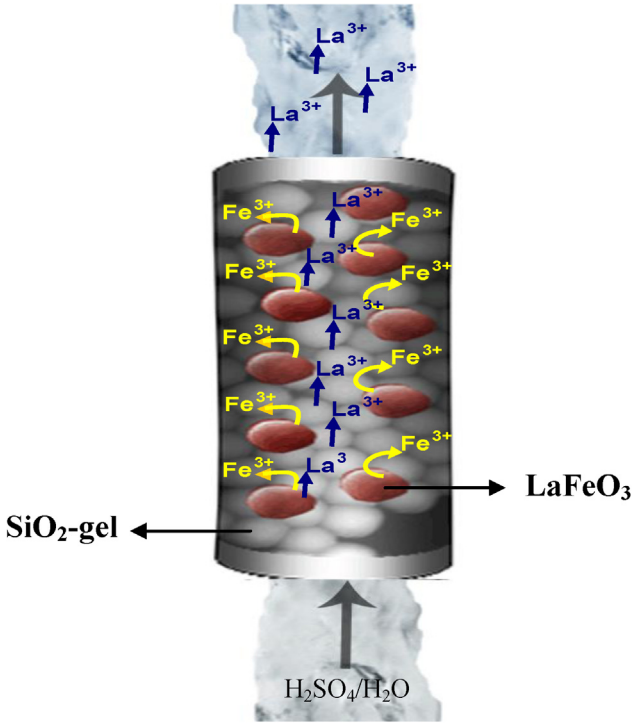

Scheme 1. SED of iron in continuous packed reactor.

ID of 8 mm. The iron ions were grafted at the surface of silica by passing the acidic solution (H_2SO_4) up-flow through the reactor at pH_{in} = 3, 80 °C, and LHSV 6 h^{-1} for a period of 8 h (Scheme 1).

2.2. Materials characterization

Surface area, pore volume, and pore size distribution were derived from N_2 adsorption–desorption isotherms, by using conventional BET and BJH methods. The samples were outgassed under vacuum for 2 h at 250 °C, and isotherms were obtained on a NOVA-2000 (Quantachrome, Version 7.02) instrument at the temperature of liquid nitrogen. Conventional wide-angle XRD patterns were obtained with a Philips 1050/70 powder diffractometer fitted with a graphite monochromator, at 40 kV and 28 mA. Software developed by Crystal Logic was used. The data were collected in a range of 2θ values between 5° and 80° with a step size of 0.05°. Phase identification was performed by using BEDE ZDS computer search/match program coupled with the Powder Diffraction File database (2006). The crystal size was determined from the Scherrer equation $h = K\lambda/[(B^2 - \beta^2)^{0.5}\cos(2\theta/2)]$, where K = 1.000 is the shape factor, λ = 0.154 nm, β is the instrumental broadening correction, and B is the reflection broadening at corresponding 2θ.

The infrared spectra were recorded with a Nicolet Impact 460 FTIR spectrometer using KBr pellets (0.005 g sample and 0.095 g KBr), with 32 sample scans. The data were treated with OMNIC software. The EDAX elemental analysis was conducted using Quanta-200, SEM-EDAX, FEI Co. instrument. HRTEM analysis was done on a FasTEM JEOL 2010 microscope operating at 200 kV. The samples for HRTEM were prepared by depositing a drop of ethanol suspension of the solid material on a carbon-coated copper grid.XPS spectra were recorded with ESCALAB 250 ultra-high vacuum (13×10^{-13} bar) apparatus with an Al Kα X-ray source and a monochromator. Powder samples of the catalysts were pressed into a thin layer on an indium-plated grid. The spectral components of Fe 2p3/2 core were found by fitting a sum of single-component lines to the experimental data by means of nonlinear least-squares curve fitting. The single-component lines were assumed to have the shape of the sum of Cauchy and Gaussian curves, and deconvolution was performed. To correct for charging effects, all spectra were calibrated relative to a carbon 1s peak positioned at 285.0 eV.

The Raman spectra were recorded with the Jobin-Yvon LabRam HR 800 micro-Raman system, equipped with a liquid-N_2-cooled detector. The excitation source was a He–Ne laser (633 nm) with a power of 5 mW on the sample. The laser was focused with a 50× long-focal-length objective to a spot of about 2 μm. Most measurements were taken with the 600 g mm^{-1} grating and a confocal microscope with a 100 μm hole with a typical exposure time of 1 min. The spectrometer was calibrated by using the typical Si line at 520 cm^{-1}. The peaks were analyzed using LabSpec software. The instrumental resolution was about 0.6 cm^{-1}. ^{57}Fe Mössbauer effect studies were conducted with a conventional Mössbauer drive and a cryogenic system. Mössbauer spectra of Fe-containing materials were recorded at 298 K with a transmission spectrometer using a sinusoidal velocity waveform and source of ^{57}Co in a rhodium matrix. Peak positions and isomer shifts of all spectra are reported with respect to metallic iron. The EPR spectrum was obtained with a Bruker EMX Plus X-band spectrometer. Typical recording conditions were: microwave frequency ca. 9.85 GHz, magnetic field sweep range 6000 G, modulation frequency 100 kHz, modulation amplitude 4.0 G, sweep time 30 s. Spectrum were taken at room temperature.

2.3. Catalytic experiments

The performance of catalysts for the degradation of phenol by means of CWPO was tested in an up-flow fixed bed reactor similar to that used in [7] (reactor ID 0.8 cm, length 18 cm, the length of catalysts layer 6–7 cm.). The test was carried out at 80 °C and LHSV of 6 h^{-1}. The aqueous solution that contained 200 ppmw phenol (Riedel de-Haën) and 1300 ppmw hydrogen peroxide (Acros Organics, 34%) corresponding to 30% excess relative to the stoichiometric amount needed for complete mineralization of phenol to (CO_2/H_2O: H_2O_2/PhOH = 14) after adjusting the pH = 4.0 by H_2SO_4 was fed to the reactor with an HPLC pump. In experiments using $LaFeO_3$–SiO_2-gel and $LaFeO_3$-quartz mixtures the LHSV was kept at 6 h^{-1} relative to the total volume of loaded mixtures.

The axial pH profiles during phenol CWPO at LHSV = 6 h^{-1} were obtained by measuring the pH at the reactor outlet running the feed water with pH_{in} = 4.0 at different LHSV that varied between 60 and 30 h^{-1}. This yielded pH values corresponded to the points of catalysts layer located at distances of 10 –50% of the total catalysts layers length from the inlet point. In order to minimize the effect of catalysts chemical transformations on pH profiles for measurements at every LHSV was used a fresh catalysts batch.

The phenol and TOC conversions were calculated according to Eqs. (8) and (9):

$$X_{PhOH} = [(C_{PhOHin} - C_{PhOHout})/C_{PhOHin}] \times 100\% \quad (8)$$

$$X_{TOC} = [(C_{TOCin} - C_{TOCout})/C_{TOCin}] \times 100\% \quad (9)$$

where $C_{PhOH(TOC)in/out}$ – concentrations of phenol or TOC (ppmw)at the reactors in- and outlet. The H_2O_2 stoichiometric efficiency was calculated according to Eq (10);

$$H_2O_{2StEf} = [H_2O_{2consumed}/H_2O_{2converted}] \times 100\% \quad (10)$$

where $H_2O_{2consumed}$ is amount of H_2O_2 (mmol) needed for complete mineralization of phenol according to measured TOC conversion and $H_2O_{2converted}$ total amount of H_2O_2 (mmol) disappeared from the solution after passing the catalyst layer. The last figure was calculated based on the difference of H_2O_2 concentrations at the reactors in-/outlet.

Two blank experiments were conducted as references in phenol CWPO. In the first experiment the standard 200 ppmw

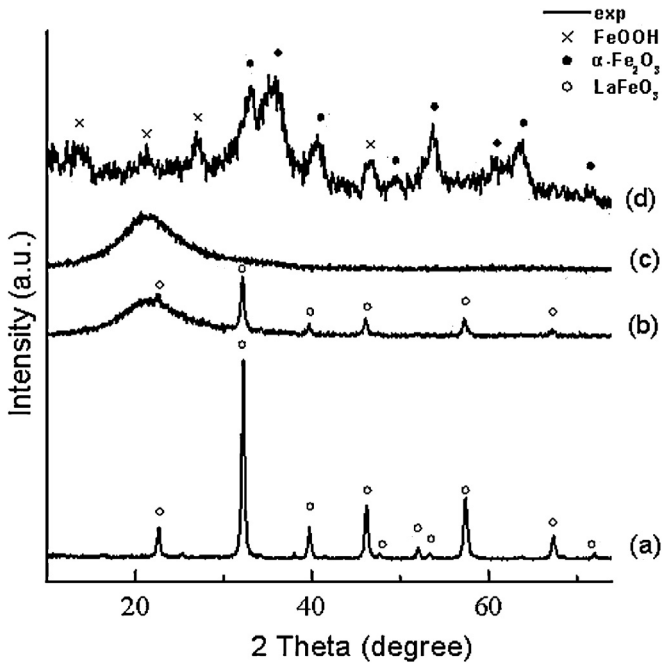

Fig. 1. XRD patterns of (a) LaFeO3; (b) $LaFeO_3$–SiO_2-gel mixture before SED; (c) 2 wt% Fe/SiO_2 ($LaFeO_3$–SiO_2-gel mixture after SED) and (d) Fe_2O_3–FeOOH–NP ($LaFeO_3$ after SED).

PhOH- 1300 ppmw H_2O_2–H_2O solution at pH_{in} = 4.0 was fed to the reactor loaded with 3 cm^3 of pure Silica-gel at LHSV = 6 h^{-1}. This yielded 92% phenol conversion and 30% conversion of TOC. In the second experiment to the standard solution was added $FeCl_3$ salt at amount corresponding to concentration of Fe-ions 60 ppmw – the maximal Fe concentration observed in reactor outlet water in this study. This yielded >99% conversion of phenol and 50% conversion of TOC.

The treated water samples taken after periods of time were analyzed for contents of phenol and products of its partial oxidation (HPLC-MS method, YMC-Pack ODS-AQ column, GBC Co. LC-1205 Instrument), TOC (Instrument TOC-VCPN Shimadzu Co.), H_2O_2 (reaction of aqueous solution with KI followed by titration with $Na_2S_2O_3$ [18]) and amount of leached iron and La (ICP, Perkin Elmer, Optima 3000).

3. Results and discussion

3.1. The state of iron in oxide materials produced by SED method

Wide-angle XRD patterns of materials $LaFeO_3$, 2 wt% Fe/SiO_2, Fe_2O_3–FeOOH–NP and their physicochemical properties are shown in Fig. 1 and Table 1, respectively. The XRD patterns show that synthesized perovskite is a pure phase with an orthorhombic structure, the diffraction data are in good agreement with JCPDS card of $LaFeO_3$ (JCPDS 74-2203). It has surface area of 41 m^2g^{-1} and the average particle size was 20 nm as determined from the XRD pattern parameters according the Scherrer equation. The XRD analysis showed that reflections corresponding to $LaFeO_3$ in initial [$LaFeO_3$–SiO_2-gel] mixture disappeared after implementing SED technique leaving only amorphous hump of SiO_2 centered at $2\theta = 23^\circ$ for 2 wt% Fe/SiO_2 sample (Fig. 1). Implementation of SED technique in the absence of silica yielded a crystalline material Fe_2O_3–FeOOH–NP containing 4.5 nm Fe_2O_3 nanoparticles of globular shape and needles of 4 nm FeOOH phase (Fig. 2a and b). It contained <2 at% of residual La in agreement with previous observation about preferential leaching out of La from $LaFeO_3$ in acidic solution [19]. The XRD patterns characteristic for amorphous material are evident for existing of iron component detected by chemical analysis in 2 wt% Fe/SiO_2-SED sample not in form of crystalline iron oxide and/or hydroxide particles further confirmed by HRTEM (not shown). This together with the absence of La in 2 wt% Fe/SiO_2-SED sample can be explained by the fact that in presence of silica-gel the chemical interaction between sulphuric acid and perovskite phase alters from reactions (6), (7) to reactions (2)–(4) yielding isolated iron ions at the surface of silica particles.

In order to confirm it the 2 wt% Fe/SiO_2 sample prepared through SED technique was further characterized by Mössbauer spectroscopy, XPS, UV Raman, FT-IR and ESR. Mössbauer spectra of $LaFeO_3$ and 2 wt%Fe/SiO_2 prepared through SED technique are shown in Fig. S1. At room temperature the orthoferrite $LaFeO_3$ perovskite revealed the classical antiferromagnetic sextet in ^{57}Fe Mössbauer spectra with slightly broadened absorption lines (Fig. S1a). The hyperfine field distribution is probably due to small $LaFeO_3$ particles. The derived mean hyperfine field is 51.4 T. The isomer shift of +0.26(1) mm/s indicates typical octahedrally coordinated Fe^{3+} ions with a negligible quadrupole interaction. After acid treatment of $LaFeO_3$–SiO_2 mixture the characteristic peaks of parent $LaFeO_3$ in Fe/SiO_2–SED disappeared and a new iron non magnetic phase appeared (Fig. S1b) having the same IS but with increased electric field gradients leading to the observed quadrupole doublet splitting. The recorded IS is +0.25(1) mm/s and the quadrupole splitting $e^2qQ = 0.71(2)$ mm/s. As the absorption line width (FWHM = 0.25 mm/s) is rather narrow it can be concluded that the Fe ions are highly isolated as no Fe–Fe interaction was observed. At low temperatures, this phase order magnetically indicated high spin coordination through Si—O—Fe linkage [20,21]. This provides the evidence for grafting of isolated Fe(3+) ions in different environments on the silica surface.

The XPS spectra of Fe2p3/2 core for selected iron containing samples (Fig. S2) are asymmetric with a tail extending in the high BE and maxima at BE 711–712 eV ascribed to Fe(3+) ions [22,23]. The broadening of peaks in samples (a) and (c) is attributed to the presence of different iron ions environment in two types of oxide particles (Fe_2O_3 and FeOOH (a)) and in perovskite crystals (c) where part of Fe ions can occupy the positions of La cations. The peaks recorded with samples (b) (Fe_2O_3) and (d) (2 wt% Fe/SiO_2) are more symmetric reflecting one state of iron ions. A significant shift of BE to high values (from 711.2 to 711.8 eV) passing from (b) to (d) can reflect the difference in the environment of paramagnetic Fe^{3+} ions. The higher BE values than in bulk Fe_2O_3 indicate the strong interaction between iron and silica, in analogy with iron incorporated in the silica framework of Fe-ZSM-5 with a binding energy of 711.6 eV [24] and iron ions incorporated in the bulk of silica-gel by co-gelation with binding energy of 712.1–712.3 eV [25]. The higher electronegativity of Si (1.90) compared with Fe (1.83), possible bonding of surface iron ions with more than one (SiO)-group at silica surface: $(SiO)_2Fe$—OH, $(SiO)_3Fe$ and formation of surface species with double-bonded oxygen atoms: SiO—Fe═O, can be responsible for the higher effective positive charging of Fe-ions in 2 wt% Fe/SiO_2 catalyst reflected by higher BE of Fe2p3/2 electrons.

Fig. S3 shows the UV Raman spectra of iron containing materials excited by 325 nm line. Three Raman bands at 490, 800 and 978 cm^{-1} are observed in the spectrum of pure silica. The band at 490 cm^{-1} is related to the three and four silane rings and the band at 800 cm^{-1} to the vibration mode of siloxane link. The band at 978 cm^{-1} is associated to the Si—O—Si bond near the framework iron species or other defect site such as surface silanols groups. Compared with the pure silica, a new band at 1075 cm^{-1} is detected for iron grafted silica material. This band is assigned to Fe—O—Si asymmetric stretching mode of the isolated iron ions over the silica [26]. The nature Si—O—Fe linkage in 2 wt% Fe/SiO_2

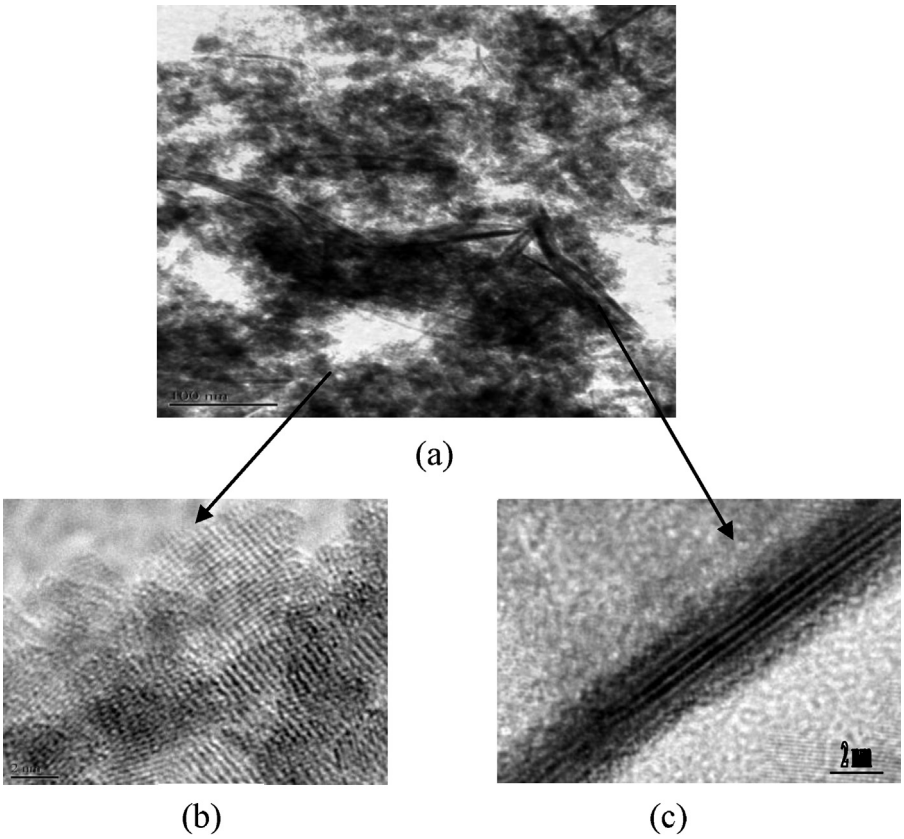

Fig. 2. HR-TEM images of (a) Fe_2O_3–FeOOH–NP, (b) Fe_2O_3–NP and (c) FeOOH–NP.

material was further verified by analysis of FT-IR spectra shown in Fig. S4. The disappearance of the peak at 970 cm^{-1} in 2 wt% Fe/SiO_2 compared to parent SiO_2 which is assigned to the presence of uncondensed Si—OH groups clearly establishes the participation of silanols in grafting of iron ions [27] thereby confirming the presence of Si—O—Fe. The coordination environment of Fe(III) in the 2 wt% Fe/SiO_2 was also elucidated by room temperature X band ESR spectroscopy (Fig. S5). The spectrum shows signal at $g = 2.0$ that indicate the presence of undistorted tetrahedral or octahedral Fe^{3+} sites [28]. Such signal has regularly been observed for isolated iron ions incorporated into silica [28,29] and zeolites [30]. There is no evidence for iron oxide cluster in this sample as these are expected to exhibit g values of 2.2–2.5 [28,31,32].

From all the above characterization results it is possible to conclude that the iron sites grafted over silica-gel through SED technique possess isolated Fe^{3+} sites. But it remained not clear the exact state of iron ions adsorbed at silica surface. The negligible residual concentration of iron (3.4 ppmw, 1.5%) measured in supernatant solution after pH equilibration in SED experiment is evident for about complete shifting of the adsorption equilibrium defined by reaction (5) to the right at selected conditions – 98.5% of iron inserted as $LaFeO_3$ was absorbed by silica as isolated metal ions. Based on surface concentration of silanols in used commercial SiO_2-gel measured as 0.68 mmol/g the maximal loading of iron after establishment of adsorption equilibrium is determined by the state of adsorbed Fe(3+) ions. Assuming the participation of all detected silanols in binding of Fe(3+) ions, calculations based on Eqs. (2)–(4) yielded 1.3 wt% Fe in form of $Fe(SiO)_3$, 2.0 wt% Fe in form of HO—$Fe(SiO)_2$ and 3.7 wt% Fe in form of O═Fe—SiO. The experimental value of 2.0 wt% can be evident for HO—$Fe(SiO)_2$ as a predominant state of surface iron ions.

3.2. Catalytic performance of iron-oxide materials prepared by SED method in CWPO of phenol

The TOC conversion in CWPO of phenol with catalytic materials prepared by SED method and with two reference materials – Fe_2O_3–FeOOH–NP and pure $LaFeO_3$, is shown in Fig. 3 as a function of run time. The characteristics of catalytic materials used in this study are listed in Table 1. 2wt% Fe/SiO_2 catalyst containing isolated iron sites yielded initial TOC conversion of 67–63% for a period of 12 h. After 20 h of running the water treatment with this catalytic material TOC conversion significantly decreased and attained a level corresponding to homogeneous (non-catalytic) CWPO of phenol at 25–30 h of run. Analysis of iron in the treated water revealed that the reason for deactivation is leaching of the active metal from silica support. The amount of iron leached out from the 2 wt% Fe/SiO_2 catalyst decreased with increasing of run time that corresponded to diminishing of its concentration in treated water from 63 to 2 ppmw that taking into account the total amount of

Table 1
Physicochemical properties of catalytic materials.

Catalytic material	Fe content (wt%)	Surface area (m^2/g)	Pore volume (cm^3/g)	Pore diameter (nm)
$LaFeO_3$	23.0	41	0.2	19
2 wt% Fe/SiO_2	2.0	298	1.1	15
Fe_2O_3–FeOOH–NP	66.5	180	0.6	13

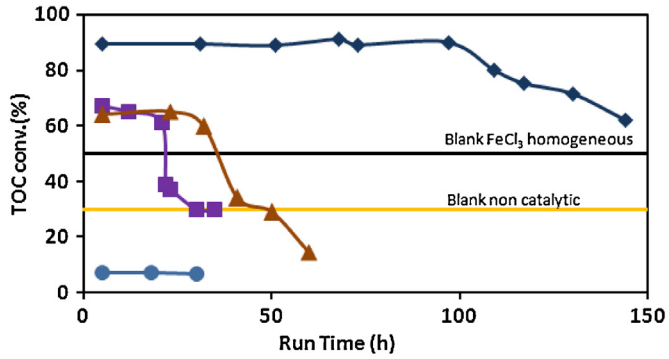

Fig. 3. TOC conversions measured with iron catalysts in CWPO of phenol: (♦) 6 wt% Fe($LaFeO_3$)–SiO_2, (■) 2 wt% Fe/SiO_2, (▲) $LaFeO_3$/Quartz (●) Fe_2O_3–FeOOH–NP. T = 80 °C; LHSV = 6 h^{-1}, [PhOH] = 200 ppm, H_2O_2/PhOH = 1.3 Stoich., pH_{in} = 4.0.

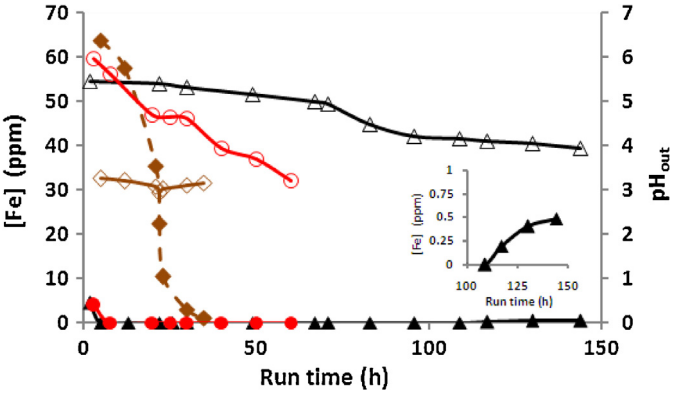

Fig. 4. Effluent water pH and leached iron concentration profiles measured in CWPO of phenol: (closed symbols: [Fe]; open symbols: pH): (▲) 6wt%Fe($LaFeO_3$)–SiO_2, (♦) 2 wt% Fe/SiO_2,(●) $LaFeO_3$/Quartz. T = 80 °C; LHSV = 6 h^{-1}, [PhOH] = 200 ppm, H_2O_2/PhOH = 1.3 Stoich., pH_{in} = 4.0.

passed water corresponds to leaching out of 85% of iron (Fig. 4). The latter reflected the lowering of iron loading in catalyst from 2.0 to 0.3 wt%. The activity of this material at the beginning of run is higher than that of homogeneous Fe catalysts dissolved at amount corresponding to concentration of leached iron: X_{TOC} = 67% versus 50% in the corresponding blank experiment.

The reason for strong leaching of iron ions from silica at phenol CWPO conditions is not straightforward since in SED experiments iron ions on the contrary were adsorbed at silica surface even at lower pH than pH_{in} in catalytic test. Measuring the axial pH profile in the reactor during catalysts testing (Fig. 5, curve 1) and analysis of the products of phenol partial oxidation obtained at high

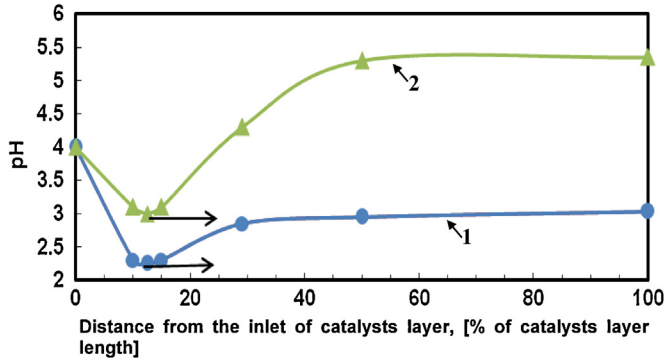

Fig. 5. Axial pH profiles measured in testing experiments with 2 wt% Fe/SiO_2 (1) and 6 wt% Fe ($LaFeO_3$)–SiO_2 (2) materials.

LHSV showed that leaching of iron ions from 2 wt% Fe/SiO_2 catalytic material is caused by formation of carboxylic compounds at the front of catalysts layer. In experiment conducted at LHSV = 60 h^{-1} the composition of treated water collected at the reactor outlet is equal to that established in the reactor working at standard LHSV = 6 h^{-1} after passing 10% of the catalysts bed. The phenol conversion measured at LHSV = 60 h^{-1} was 86% while the TOC conversion – only 15%, evident for the partial oxidation of phenol. The partial oxidation of phenol at this point yielded a set of intermediate compounds including carboxylic acids: maleic and its isomer fumaric acid being the primary products of phenol ring opening as well as acetic, oxalic and formic acids resistant to mineralization at low resident time. Formation of these intermediates caused a significant decrease of the pH from 4.0 at reactor inlet to 2.2 at this point of the catalysts layer. Further moving along the catalysts bed caused increasing of pH up to 3.1 at the reactor outlet due to oxidative conversion and mineralization of the part of these acids. Decreasing of pH at the reactor inlet together with interaction of adsorbed iron ions with carboxylic acids strongly shifts the adsorption equilibrium toward iron desorption via complexation and reductive dissolution [33,34] detected as iron leaching. With increasing of run time the axial pH profile in the catalysts bed changes in such a way that the position of the point where the pH passes through a minimum value (Fig. 5) is shifted up toward the reactors outlet. The reason for it is leaching out of iron ions from lower parts of the catalysts bed, thus reducing the catalytic activity of these parts and diminishing production of acidic intermediates. The stoichiometric efficiency of H_2O_2 with 2 wt% Fe/SiO_2 material was high – 84.5%. The high H_2O_2 stoichiometric efficiency is generally observed in Fenton oxidation reactions where hydrogen peroxide is catalytically decomposed by iron ions according to the Haber–Weiss mechanism yielding $^{\bullet}OH$ radicals [11,12].

The mixed Fe-oxide–oxide–hydroxide material (Fe_2O_3–FeOOH–NP) displayed very low activity in phenol mineralization (Fig. 3) at reasonable phenol conversion (Table 2). Phenol was mainly transferred to catechol and hydroquinone with very low TOC removal of 5%. The low H_2O_2 stoichiometric efficiency of 3.8% detected in this test is consistent with earlier observations reported by several groups for CWPO of different organic contaminants with bulk Fe-oxides and hydroxides [11,35,36]. It may be attributed to rapid scavenging of $^{\bullet}OH$ radicals at the iron oxide surface due to low distance between surface iron ions [35] and/or non-selective decomposition of hydrogen peroxide by bulk hematite and goethite according to the two-electron disproportionation route [37]. This yields molecular oxygen not active in phenol oxidation at selected testing conditions. Such behavior is characteristic for H_2O_2 decomposition catalyzed by bulk nanocrystalline iron oxides–hydroxides producing $^{\bullet}OH$ radicals [38] and molecular oxygen with similar rates at pH 4–7 [37,39,40]. It yielded TOC conversions even lower than were observed in blank experiments where $^{\bullet}OH$ radicals were not scavenged and H_2O_2 was not converted to O_2—H_2O species.

Pure $LaFeO_3$ mixed with chemically inert quartz particles displayed initial catalytic activity and high H_2O_2 efficiency comparable with that of 2 wt% Fe/SiO_2 material for a period of about 30 h (Fig. 3) without iron leaching (Fig. 4). This is consistent with observations reported in [15] where $LaFeO_3$ material demonstrated high PhOH and TOC conversions in a batch reactor without significant iron leaching. But La was leached out from the beginning of run (30–35 ppmw La was detected in the treated water at this period) due decomposition of perovskite that reacted with sulphuric acid according to reactions (6)–(7). The formed Fe_2O_3–FeOOH were deposited on quartz particles with no leaching of iron and detected by XRD after discharging the spent catalytic material. Accumulation of Fe_2O_3–FeOOH–NP in catalysts layer at the end of run caused decreasing of TOC conversion below that observed in blank

Table 2
Performance and iron concentration in treated water measured with tested catalysts at various time intervals in the CWPO of phenol at $T = 80\,^{\circ}C$; LHSV = 6 h^{-1}, [PhOH] = 200 ppmw, H_2O_2/PhOH = 1.3 Stoich., pH_{in} = 4.0.

Catalytic material	Outlet [Fe] ppmw in treated water after following run time (h):				X_{TOC} after 25 h (%)	X_{phenol} after 25 h (%)	X_{H2O2} after 25 h (%)	H_2O_2 stoichiometric efficiency after 25 h (%)
	25	50	75	100				
6 wt% Fe($LaFeO_3$)–SiO_2	<0.05	<0.05	<0.05	<0.05	91	100	84.9	82.3
2 wt% Fe/SiO_2	10	–	–	–	39	100	35.3	84.5
$LaFeO_3$/quartz	<0.05	<0.05	–	–	65	100	69.0	78.0
Fe_2O_3–FeOOH–NP	<0.05	<0.05	–	–	5	60	100	3.8

experiments with decreasing of H_2O_2 stoichiometric efficiency as detected for pure Fe_2O_3–FeOOH–NP.

The most significant effect was observed in testing of 6 wt% Fe($LaFeO_3$)–SiO_2 material that contained excess of iron compared with the adsorption capacity of silica component according to its silanols concentration. The excess of iron was used in order to compensate possible leaching of iron with the run time by iron continuously released from the perovskite. This mixed catalytic material demonstrated high TOC conversion of 90% with less than 0.05ppmw of leached iron in effluent water (Table 2) during the testing period of 100 h without deactivation (Fig. 3). It displayed a hydrogen peroxide stoichiometric efficiency of 82.3% (Table 2) and the pH_{out} of effluent water remained in range from 5.3 to 4.2 for 100 h of reaction (Fig. 4). The lanthanum ions were leached out from the catalyst bed during the run. Their concentration in treated water was ~35 ppmw up to 85 h of run and then started to go down to 20 ppmw at 100 h and 7 ppm at 140 h. After this period, the pH at the reactor outlet decreased to less than 4.0 and leached iron appeared in the treated water at amounts of 0.2–0.5 ppm (inset in Fig. 4). The TOC conversion started to drop after 110 h of run up to 60% at the run time of 140 h due to deactivation of the mixed catalytic material (Figs. 3 and 4). These observations can be explained by a model assuming a diverse dynamics of the state of heterogeneous Fenton catalytic system along the catalysts bed in CWPO of phenol.

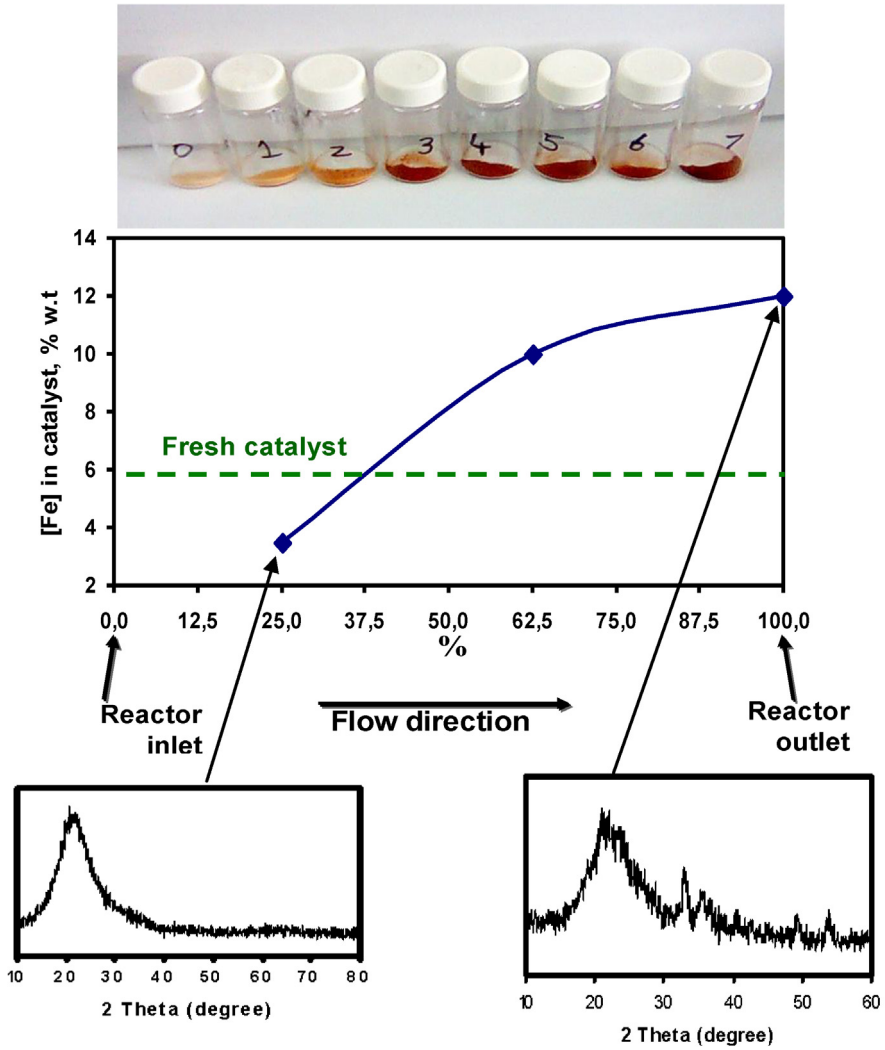

Fig. 6. Distribution of iron in spent 6 wt% Fe($LaFeO_3$)–SiO_2 material along the catalysts layer after 120 h of run in CWPO of phenol: $T = 80\,^{\circ}C$; LHSV = 6 h^{-1}, [PhOH] = 200 ppmw, H_2O_2/PhOH = 1.3 Stoich., pH_{in} = 4.0.

During the activation period modeling the conditions of iron SED a small part of perovskite phase was decomposed and silica-gel particles were loaded with iron ions according to reactions (2)–(4). This produced a two-phase mixed catalysts bed which components about equally contributed to the total catalytic activity (the initial TOC conversions measured separately with 2 wt% Fe/SiO_2 and LaFeO3/Quartz where 67–63 and 63–65%, respectively). As expected, this yielded the total TOC conversion of 90% – significantly higher than it was measured with individual components of mixed catalytic material (Fig. 3). Less straightforward is the explanation of high stability of this mixed catalytic material much beyond to that measured for individual components in previous runs and absence of leached iron in treated water during the testing period of 100 h.

The axial pH profile in the catalysts bed measured at the beginning of the run in this case displayed the same shape (Fig. 5, curve 2) as it was established in testing of 2 wt% Fe/SiO_2 material. But all the pH values were higher by 0.8–2.3 units. This increase of pH should be a sequence of reaction between $LaFeO_3$ and sulphuric acid entering the catalyst bed with acidic solution as well as with carboxylic acids – intermediates of phenol oxidation, so that perovskite phase acts also as a buffer. As a result the iron ions leached from silica-gel component at low pH corresponding to the minimum point at the axial pH profile curve became condensed and precipitates as iron oxide–hydroxides at higher pH in upper layers of the catalyst bed and do not leave the reactor. Due to intensive decomposition and disappearance of $LaFeO_3$ in lower catalysts layers the position of the minimum pH point should shift up favoring the perovskite decomposition in upper layers of catalysts bed. It compensates the iron leached out from the silica component. This explains the increasing of the stability of catalysts performance compared with 2 wt% Fe/SiO_2 material and absence of leached iron at the reactor outlet. After all perovskite is decomposed, the residual iron adsorbed on silica in upper layers of the catalyst bed as isolated iron ions is attacked by the acid protons present in the water and produced by phenol partial oxidation to carboxylic acids causing iron leaching. This is a reason for deactivation of the mixed catalytic material at the end of the run.

This concept is confirmed through analyzing the spent mixed catalyst 6 wt% $Fe(LaFeO_3)$–SiO_2 with XRD and EDS after 120 h of reaction. Fig. 6 shows photograph of spent catalyst collected in various vials as it was discharged starting from bottom (vial No. 0) to top (vial No. 7) of the reactor. Increase of color from white to light brown, XRD patterns characteristic for amorphous silica and absence (vial No.1) or lower iron content in the front of catalysts layer (vials No.1 and 2) compared with the initial iron content of 6 wt% clearly indicate the displacement of iron ions from the bottom part of catalysts layer. Intensification of brown color from middle to top parts of the layer of spent catalyst and increasing of iron content beyond 6 wt% are clearly evident from the Fig. 6. Appearance of reflections characteristic for Fe_2O_3 nanoparticles with diameter of 15 nm in XRD patterns and continuous increase of iron content toward to catalysts layer outlet implies that all the iron leached at the bottom of the catalysts layer was captured at its upper parts through condensation. The above observations confirm the proposed dynamic model explaining the strong synergistic effect that appeared in CWPO of phenol after mechanical mixing of $LaFeO_3$ and silica-gel materials. It can serve as a basis for future investigations aiming proper reactors design for continuous feeding of iron and implementation of other solid buffers for highly efficient cleaning of contaminated wastewater at mild conditions.

4. Conclusions

A new method defined as selective extraction deposition (SED) was proposed to prepare heterogeneous Fenton catalyst-isolated iron sites at silica surface, which state was confirmed by characterization results. This well defined state of iron is a sequence of low residence time of iron ions extracted from $LaFeO_3$ perovskite precursor in acidic aqueous solution. The quick adsorption of Fe ions (co-condensation with surface silanols) prevents their self-condensation into oxide-hydroxide clusters and nanoparticles. This catalyst showed reasonable catalytic activity in CWPO of phenol in continuous plug flow reactor. However leaching of iron caused its rapid deactivation. It was demonstrated that mixing of $LaFeO_3$ with silica-gel gives an advanced catalytic material with high activity (TOC removal of 90%) and stability. This is attributed to dynamic behavior of iron including its SED–leaching–condensation along the catalysts layer. The finding has a potential environmental impact enabling the development of efficient catalytic filters for industrial wastewater contaminated with organics by tailoring the solid precursor of iron ions, axial pH profile inside the reactor and the nature of the sorbent/stabilizer for iron ions.

Acknowledgment

This study was supported by Israeli Ministry of Science and Technology – MOST (Grant WT 1002) and DST-SERB Fast Track (Sanction No. SR/FT/CS-138/2011), Government of India, New Delhi. The authors gratefully acknowledge Dr. N. Froumin, Dr. V. Ezersky and Dr. A. Erenburg for conducting the materials characterization using, respectively, XPS, HRTEM and XRD methods.

Appendix A. Supplementary data

Supplementary data associated with this article can be found, in the online version, at http://dx.doi.org/10.1016/j.apcatb.2013.02.040.

References

[1] P. Bautista, A.F. Mohedano, J.A. Casas, J.A. Zazo, J.J. Rodriguez, Journal of Chemical Technology and Biotechnology 83 (2008) 1323–1338.
[2] P.R. Gogate, A.B. Pandit, Advances in Environmental Research 8 (2004) 501–551.
[3] S. Perathoner, G. Centi, Topics in Catalysis 33 (2005) 207–224.
[4] J. Barrault, M. Abdellaoui, C. Bouchoule, A. Majeste, J.M. Tatiboute, A. Louloudi, N. Papayannakos, N.H. Gangas, Applied Catalysis B 27 (2000) L225–L235.
[5] E. Guelou, J. Barrault, J. Fournier, J.M. Tatibouet, Applied Catalysis B 44 (2003) 1–8.
[6] A. Quintanilla, A.F. Fraile, J.A. Casas, J.J. Rodriguez, Journal of Hazardous Materials 146 (2007) 582–588.
[7] F. Martinez, J.A. Melero, J.A. Botas, M.I. Pariente, R. Molina, Industrial and Engineering Chemistry Research 46 (2007) 4396–4404.
[8] J.A. Botas, J.A. Melero, F. Martinez, M.I. Pariente, Catalysis Today 149 (2010) 334–340.
[9] M.A. anderson, M.H. Palm-Gennen, P.N. Renard, C. Defosse, P.G. Rouxhet, Journal of Colloid and Interface Science 102 (1984) 328–336.
[10] R. Prucek, M. Hermanek, R. Zboril, Applied Catalysis A 366 (2009) 325–332.
[11] A.L-T. Pham, C. Lee, F.M. Doyle, D.L. Sedlak, Environmental Science and Technology 43 (2009) 8930–8935.
[12] J.J. Pignatello, E. Oliveros, A. MacKay, Critical Reviews in Environmental Science and Technology 36 (2006) 1–84.
[13] C. Nozaki, C. Lugmair, A.T. Bell, T.D. Tilley, Journal of the American Chemical Society 124 (2002) 13194–13203.
[14] Y. Li, H. Xia, F. Fan, Z. Feng, R.A. van Santen, E.J.M. Hensen, C. Li, Chemical Communications (2008) 774–776.
[15] J. Faye, E. Guélou, J. Barrault, J.M. Tatibouët, Topics in Catalysis 52 (2009) 1211–1219.
[16] D.L. Dugger, J.H. Stanton, B.N. Irby, B.L. McConnell, W.W. Cummings, R.W. Maatman, Journal of Physical Chemistry 68 (1964) 757–760.
[17] A. Rahman, P. Vejayakumaran, C.S. Sipaut, J. Ismail, C.K. Chee, Materials Chemistry and Physics 114 (2009) 328–332.
[18] E. Graf, J.T. Penniston, Clinical Chemistry 26 (1980) 658–660.
[19] M. Yang, A. Xu, H. Du, C. Sun, C. Li, Journal of Hazardous Materials 139 (2007) 86–92.
[20] G. Calis, P. Frenken, E. de Boer, A. Swolfs, M.A. Hefni, Zeolites 7 (1987) 319–326.
[21] A.A. Jara, S. Goldberg, M.L. Mora, Journal of Colloid and Interface Science 292 (2005) 160–170.
[22] D.D. Hawn, B.M. DeKoven, Surface and Interface Analysis 10 (1987) 63–74.
[23] J. Janas, J. Gurgul, R.P. Socha, T. Shishido, M. Che, S. Dzwigaj, Applied Catalysis B: Environmental 91 (2009) 113–122.

[24] R.B. Borade, A. Adnot, S. Kaliaguine, Zeolites 11 (1991) 710–719.
[25] P. Fabrizioli, T. Burgi, M. Burgener, S. van Doorslaer, A. Baiker, Journal of Materials Chemistry 12 (2002) 619–630.
[26] Y-M. Liu, J. Xu, L. He, Y. Cao, H-Y. He, D-Y. Zhao, J-H. Zhuang, K-N. Fan, Journal of Physical Chemistry C 112 (2008) 16575–16583.
[27] G. Satishkumar, L. Titelman, M.V. Landau, Journal of Solid State Chemistry 182 (2009) 2822–2828.
[28] D. Goldfarb, M. Bernard, K.G. Strohmainer, D.E.W. Vaughan, H. Thomann, Journal of the American Chemical Society 116 (1994) 6344–6353.
[29] S. Bordiga, R. Buzzoni, F. Geobaldo, C. Lamberti, E. Giamello, A. Zecchira, G. Leofanti, G. Petrini, G. Tozzola, G. Vlaic, Journal of Catalysis 158 (1996) 486–501.
[30] A. Ribera, I.W.C.E. Arends, S. de Vries, J.P.- Pamı'rez, R.A. Sheldon, Journal of Catalysis 195 (2000) 287–290.
[31] B.M. Wechuysen, D. Wang, M.P.R. Rosynek, J.H. Lunsford, Angewandte Chemie International Edition 36 (1997) 2374–2376.
[32] P. Selvam, S.E. Dapurkar, S.K. Badamali, M. Murugasan, H. Kuwano, Catalysis Today 68 (2001) 69–74.
[33] M.Pera-Titus, V.Garsia-Molina, M.A. Banos, J. Gimenez, S. Esplugas, Applied Catalysis B 47 (2004) 219–256.
[34] D. Panias, M. Taxiarchou, I. Paspaliaris, A. Kontopoulos, Hydrometallurgy 42 (1996) 257–265.
[35] R.L. Valentine, H.C.A. Wang, Journal of Environment Engineering 124 (1998) 31–38.
[36] H.-H. Huang, M.-C. Lu, J.-N. Chen, Water Research 35 (2001) 2291–2299.
[37] Y.N. Lee, R.M. Lago, J.L.C. Fierro, J. Gonzales, Applied Catalysis A 215 (2001) 245–256.
[38] A.L-T. Pham, F.M. Doyle, D.L. Sedlak, Environmental Science and Technology 46 (2012) 1055–1062.
[39] R.J. Watts, M.K. Foget, S-H. Kong, A.L. Teel, Journal of Hazardous Materials 69 (1999) 229–243.
[40] M.A.A. Schoonen, C.A. Cohn, E. Roemer, R. Laffers, S.R. Simon, R. Sanford, T.O'. Riordan, Reviews in Minerology & Geochemistry 64 (2006) 179–221.